DALTON
FULL PAPER

Probing the Lewis basicity of the metalloligand $[Pt_2(\mu\text{-}Se)_2(PPh_3)_4]$ on tin substrates by electrospray mass spectrometry

Jeremy S. L. Yeo,[a] Jagadese J. Vittal,[a] William Henderson *[b] and T. S. Andy Hor *[a]

[a] *Department of Chemistry, National University of Singapore, 3 Science Drive 3, Singapore 117543. E-mail: chmandyh@nus.edu.sg*
[b] *Department of Chemistry, University of Waikato, Private Bag 3105, Hamilton, New Zealand. E-mail: w.henderson@waikato.ac.nz*

Received 23rd August 2000, Accepted 20th November 2000
First published as an Advance Article on the web 8th January 2001

Electrospray Mass Spectrometry (ESMS) has been used as a tool to probe the reactivity of $[Pt_2(\mu\text{-}Se)_2(PPh_3)_4]$ with tin(IV) substrates, which leads to the formation of charged coordination complexes *via* loss of halides. The metal substrates used in the displacement reactions are SnR_xCl_{4-x} ($x = 1$, R = Me, Bu or Ph; $x = 2$, R = Me, Bu, Et or Ph; $x = 3$, R = Me, Ph) and $Sn(CH_2Ph)_2Br_2$. Most of these reactions gave both mono- and di-cations through displacement of one and two halides respectively by $[Pt_2(\mu\text{-}Se)_2(PPh_3)_4]$. ESMS was also used to monitor the progress of reactions. The products, upon isolation, were also characterized by NMR and X-ray single crystal crystallographic analysis. The crystal structures of the aggregates $[Pt_2(\mu_3\text{-}Se)_2(PPh_3)_4(SnBuCl_2)][PF_6]$, $[Pt_2(\mu_3\text{-}Se)_2(PPh_3)_4(SnBu_2Cl)][PF_6]$ and $[Pt_2(\mu_3\text{-}Se)_2(PPh_3)_4(SnMe_2Cl)][PF_6]$ are reported and discussed.

Introduction

Mass spectrometry has been applied to the characterization of inorganic and organometallic substances for many years, but the traditional electron impact method of ionization is generally limited to thermally robust, neutral compounds of low molecular mass.[1] Electrospray mass spectrometry (ESMS) is a relatively new ionization method introduced in the mid-1980s, largely by Fenn *et al.*[2] Its gentle ionization process easily supersedes the more established mass spectrometric techniques, including fast atom bombardment (FAB). ESMS was quickly exploited by researchers working with biomolecules because proteins and other high-mass, thermally sensitive substrates could readily be analysed.[2a,3] Only recently there has been corresponding interest from inorganic chemists.[4,5] Our main interests in the area of inorganic ESMS lie in the development of the technique to monitor chemical reactions. In a parallel study, we have demonstrated the utility of this technique in probing the chemistry of $[Pt_2(\mu\text{-}S)_2(PPh_3)_4]$.[6] While there is a substantial chemistry reported on $[Pt_2(\mu\text{-}S)_2(PPh_3)_4]$,[7] the coordination chemistry of the $\{Pt_2Se_2\}$ core has been little studied. The nucleophilicity of the selenide centres is poorly understood although the ability of $[Pt_2(\mu\text{-}Se)_2(PPh_3)_4]$ to interact with different metal species is potentially rich. In this paper we discuss ESMS-monitored reactions between $[Pt_2(\mu\text{-}Se)_2(PPh_3)_4]$ **1** with tin(IV) substrates. A prime objective of this work is to establish a potentially facile route to assemble heterometallic selenide aggregates and clusters which are relatively rare.[8]

Results and discussion

ESMS-monitored reactions

The reactions of the metalloligand $[Pt_2(\mu\text{-}Se)_2(PPh_3)_4]$ **1** with a range of tin(IV) complexes have been examined using ESMS. Tin has a strong affinity for both sulfur and selenium.[9] ESMS data for reactions between **1** and the tin substrates are summarized in Table 1. Although hydrolysis by the protic solvent (MeOH) on the Sn–Cl species was expected, no Sn–OMe species was detected.

Displacement of one or two labile halide through nucleophilic attack of the Se atoms of complex **1** is commonly observed, which then leads to formation of cationic aggregates. Most reactions gave both mono- and di-cations through loss of one and two ligands respectively. Di-cations became the dominant species when more substrate was added to these reaction mixtures. As the cone voltage was increased monocations were the common dominant peaks in the spectra. Cone voltages were varied up to a maximum of 80 V, beyond which fragmentation was observed. The major fragmentation route involves loss of PPh_3 ligands at high cone voltages of 60 or 80 V. Detection of peaks at *m*/*z* 799 and 1598, assigned as $[\mathbf{1} + 2H]^{2+}$ and $[\mathbf{1} + H]^+$ respectively, were normally observed when reactions did not occur, or **1** was in excess. Similar study of $[Pt(\mu\text{-}S)_2(PPh_3)_4]$ **2** gave peaks pertaining to $[\mathbf{2} + 2H]^{2+}$ and $[\mathbf{2} + H]^+$.[6]

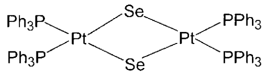

1

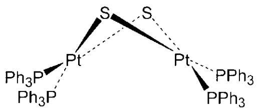

2

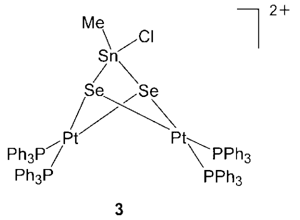

3

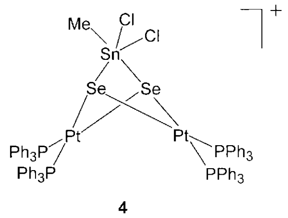

4

At low cone voltages (5–20 V) the predominant products arising from complex **1** and $SnMeCl_3$ were $[\mathbf{1}(SnMeCl)]^{2+}$ **3** and $[\mathbf{1}(SnMeCl_2)]^+$ **4** at *m*/*z* 883 and 1802 respectively. Fragmentation began at 60 V through loss of a PPh_3 ligand from $[\mathbf{1}(SnMeCl_2)]^+$ to give $[(\mathbf{1} - PPh_3)(SnMeCl_2)]^+$ (*m*/*z* 1540). At 80 V the latter became the dominant ion. Reactions of **1** with $SnRCl_3$ (R = Bu or Ph) gave very clean spectra. $[\mathbf{1}(SnRCl_2)]^+$

DOI: 10.1039/b006907h

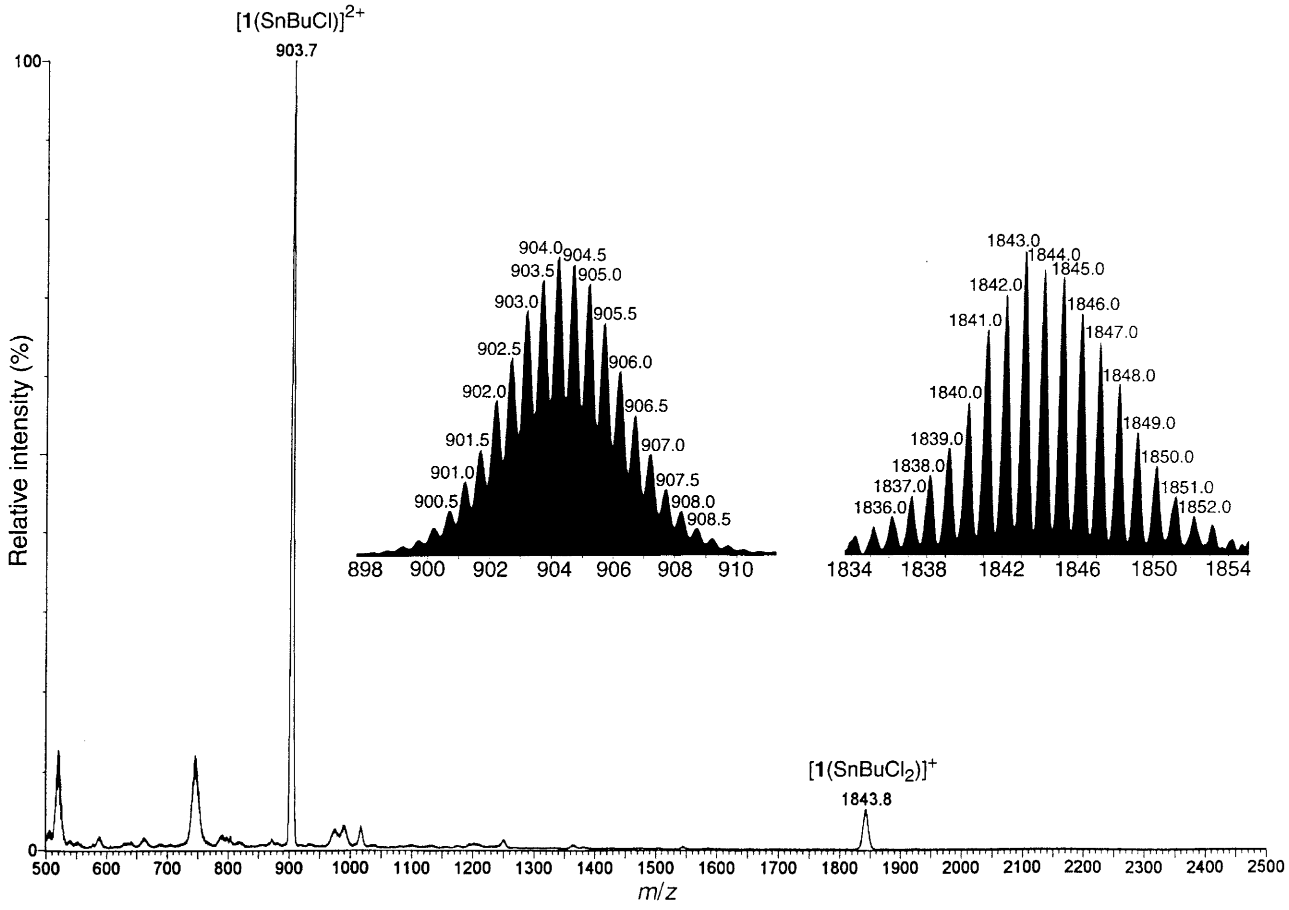

Fig. 1 Positive-ion ESMS spectrum (cone voltage 20 V) depicting the cationic species detected in the reaction between complex **1** and $SnBuCl_3$.

and $[\mathbf{1}(SnRCl)]^{2+}$ detected at low voltages (Fig. 1) gave way to $[\mathbf{1}(SnRCl_2)]^+$ at high voltages.

Parallel behavior was observed between complex **1** and $SnMe_2Cl_2$ in terms of fragmentation pattern and peak intensities of the major ions. Similarly, **1** and $SnEt_2Cl_2$ gave $[\mathbf{1}(SnEt_2)]^{2+}$ and $[\mathbf{1}(SnEt_2Cl)]^+$ between 20 and 40 V. Phosphine dissociation beginning at 60 V resulted in $[(\mathbf{1} - PPh_3)(SnEt_2)]^{2+}$ and $[(\mathbf{1} - PPh_3)(Sn)]^{2+}$ with $[\mathbf{1}(SnEt_2Cl)]^+$ still dominating as the most intense ion. Increasing the cone voltage to 80 V resulted in disappearance of all di-cations and emergence of a peak at *m/z* 1547 pertaining to $[(\mathbf{1} - PPh_3)(SnEt_2Cl)]^+$. The fragmentation pattern between **1** and $SnBu_2Cl_2$ or $SnPh_2Cl_2$ is similar. Interaction between **1** and $Sn(CH_2Ph)_2Br_2$ at low cone voltages similarly gave rise to $[\mathbf{1}(Sn(CH_2Ph)_2Br)]^+$ and $[\mathbf{1}(Sn(CH_2Ph)_2)]^{2+}$. However, at 60 V, an intense peak pertaining to $[\mathbf{1}(Sn)]^{2+}$ was observed, possibly due to fragmentation of $[\mathbf{1}(Sn(CH_2Ph)_2)]^{2+}$ as there was a corresponding drop in intensity of the latter peak. At 80 V peaks of $[\mathbf{1}(Sn(CH_2Ph)_2)]^{2+}$, $[\mathbf{1}(Sn)]^{2+}$ and $[\mathbf{1}(Sn(CH_2Ph)_2Br)]^+$ occurred at relative intensities of 4:5:50, proving that the dominance of mono-cations at high voltages is not sensitive to the alkyl or halide.

Reaction between complex **1** and $SnMe_3Cl$ is much less spontaneous compared to those of the lower methyl derivatives described above. This is consistent with the reduced Lewis acidity of $SnMe_3Cl$. At a low cone voltage (20 V), $[\mathbf{1} + 2H]^{2+}$, $[\mathbf{1} + H]^+$ and $[\mathbf{1}(SnMe_3)]^+$ were detected. $[\mathbf{1} + H]^+$ appeared as the dominant ion, even with the addition of an excess of $SnMe_3Cl$. At 40 V fragmentation began, resulting in detection of $[(\mathbf{1} - PPh_3)(SnMe_3)]^+$ by loss of a PPh_3 ligand. Further increasing the cone voltage to 60 V eliminated $[\mathbf{1} + 2H]^{2+}$, with $[\mathbf{1} + H]^+$ still dominating as the major ion. Interaction between **1** and $SnPh_3Cl$ at 20–60 V afforded $[\mathbf{1}(SnPh_3)]^+$ as the major ion, and $[\mathbf{1}(SnPh_2Cl)]^+$ and $[\mathbf{1}(SnPh_2)]^{2+}$ as the minor species (intensity ratio 20:3:8). $[\mathbf{1}(SnPh_2Cl)]^+$ which arises from $SnPh_2Cl_2$, as a contaminant, was confirmed in a ^{31}P NMR analysis (see below). At higher voltages, phosphine fragmentation intensifies, giving rise to largely $[(\mathbf{1} - PPh_3)(SnPh_2Cl)]^+$ and $[(\mathbf{1} - PPh_3)(SnPh_3)]^+$.

We decided to carry out Schlenk-flask syntheses and isolate these spectroscopically detected $\{PtSeSn^{IV}\}$ charged aggregates. The products were characterized by conventional NMR and single-crystal X-ray diffraction analyses. The results demonstrated that ESMS is valuable not only in monitoring the progress of reactions, it also provides a preliminary "screening" of the feasibility of reactions prior to lab-scale syntheses.

NMR studies

The ^{31}P NMR spectra of all $\{Pt_2Se_2Sn^{IV}\}$ aggregates synthesized were studied. ^2J(P–Se) couplings were too weak (coupled with low abundance (7.63%) of natural ^{77}Se) to be detected, under the experimental conditions employed. The presence of multi-spin systems would also split (and weaken) the selenium satellites considerably. The ^1J(Pt–P) magnitudes decrease in the order: $[\mathbf{1}(SnRCl_2)]^+$ (R = Me, Ph; 3212, 3223 Hz) > $[\mathbf{1}(SnR_2Cl)]^+$ (R = Me, Ph; 3151, 3178 Hz) > $[\mathbf{1}(SnR_3)]^+$ (R = Me, Ph; 3037, 3124 Hz). This reflects a decreasing Lewis acidity as the number of R groups increases. High acidity of the $\{SnRCl_2\}$ moiety promotes a strong coordination of the phosphine ligands on Pt. A similar trend was observed in the coordination behavior of $Pt_2(\mu\text{-}S)_2(PPh_3)_4$ **2**.[6] Reaction between **1** and $SnPh_2Cl_2$ gives cleanly $[\mathbf{1}(SnPh_2Cl)]^+$. This cationic complex forms as a by-product in a mixture containing **1** and $SnPh_3Cl$ (Fig. 2) due to the presence of $SnPh_2Cl_2$ as a trace contaminant.

Structural results

A structural analysis was carried out to investigate the effects on the $\{Pt_2Se_2\}$ core of complex **1** upon coordination to tin substrates. Crystallographic data for compounds $[Pt_2(\mu_3\text{-}Se)_2$-

Table 1 ESMS data for reactions between $[\mathrm{Pt_2(\mu\text{-}Se)_2(PPh_3)_4}]$ **1** and tin(IV) substrates

Combination	Cone voltage/V	Major ions (*m*/*z*, %)
$\mathbf{1} + \mathrm{SnMeCl_3}$	20	$[\mathbf{1}(\mathrm{SnMeCl})]^{2+}$ (883, 100), $[\mathbf{1}(\mathrm{SnMeCl_2})]^{+}$ (1802, 15)
	40	$[\mathbf{1}(\mathrm{SnMeCl})]^{2+}$ (883, 100), $[\mathbf{1}(\mathrm{SnMeCl_2})]^{+}$ (1802, 83)
	60	$[\mathbf{1}(\mathrm{SnMeCl})]^{2+}$ (883, 31), $[(\mathbf{1} - \mathrm{PPh_3})(\mathrm{SnMeCl_2})]^{+}$ (1540, 10), $[\mathbf{1}(\mathrm{SnMeCl_2})]^{+}$ (1802, 100)
	80	$[\mathbf{1}(\mathrm{SnMeCl})]^{2+}$ (883, 5), $[(\mathbf{1} - \mathrm{PPh_3})(\mathrm{SnMeCl_2})]^{+}$ (1540, 100), $[\mathbf{1}(\mathrm{SnMeCl_2})]^{+}$ (1802, 35)
$\mathbf{1} + \mathrm{SnMe_2Cl_2}$	20	$[\mathbf{1}(\mathrm{SnMe_2})]^{2+}$ (873, 100), $[\mathbf{1}(\mathrm{SnMe_2Cl})]^{+}$ (1781, 10)
	40	$[\mathbf{1}(\mathrm{SnMe_2})]^{2+}$ (873, 100), $[\mathbf{1}(\mathrm{SnMe_2Cl})]^{+}$ (1781, 80)
	60	$[\mathbf{1}(\mathrm{SnMe_2})]^{2+}$ (873, 30), $[(\mathbf{1} - \mathrm{PPh_3})(\mathrm{SnMe_2Cl})]^{+}$ (1519, 10), $[\mathbf{1}(\mathrm{SnMe_2Cl})]^{+}$ (1781, 100)
	80	$[\mathbf{1}(\mathrm{SnMe_2})]^{2+}$ (873, 9), $[(\mathbf{1} - \mathrm{PPh_3})(\mathrm{SnMe_2Cl})]^{+}$ (1519, 100), $[\mathbf{1}(\mathrm{SnMe_2Cl})]^{+}$ (1781, 25)
$\mathbf{1} + \mathrm{SnMe_3Cl}$	20	$[\mathbf{1} + 2\mathrm{H}]^{2+}$ (799, 29), $[\mathbf{1} + \mathrm{H}]^{+}$ (1598, 100), $[\mathbf{1}(\mathrm{SnMe_3})]^{+}$ (1761, 27)
	40	$[\mathbf{1} + 2\mathrm{H}]^{2+}$ (799, 5), $[\mathbf{1} + \mathrm{H}]^{+}$ (1598, 100), $[(\mathbf{1} - \mathrm{PPh_3})(\mathrm{SnMe_3})]^{+}$ (1499, 5), $[\mathbf{1}(\mathrm{SnMe_3})]^{+}$ (1761, 20)
	60	$[\mathbf{1} + \mathrm{H}]^{+}$ (1598, 100), $[(\mathbf{1} - \mathrm{PPh_3})(\mathrm{SnMe_3})]^{+}$ (1499, 12), $[\mathbf{1}(\mathrm{SnMe_3})]^{+}$ (1761, 10)
$\mathbf{1} + \mathrm{SnEt_2Cl_2}$	20	$[\mathbf{1}(\mathrm{SnEt_2})]^{2+}$ (887, 54), $[\mathbf{1}(\mathrm{SnEt_2Cl})]^{+}$ (1809, 100)
	40	$[\mathbf{1}(\mathrm{SnEt_2})]^{2+}$ (887, 41), $[\mathbf{1}(\mathrm{SnEt_2Cl})]^{+}$ (1809, 100)
	60	$[(\mathbf{1} - \mathrm{PPh_3})\mathrm{Sn}]^{2+}$ (727, 10), $[(\mathbf{1} - \mathrm{PPh_3})(\mathrm{SnEt_2})]^{2+}$ (756, 6), $[\mathbf{1}(\mathrm{SnEt_2})]^{2+}$ (887, 7), $[\mathbf{1}(\mathrm{SnEt_2Cl})]^{+}$ (1809, 100)
	80	$[(\mathbf{1} - \mathrm{PPh_3})(\mathrm{SnEt_2Cl})]^{+}$ (1547, 50), $[\mathbf{1}(\mathrm{SnEt_2Cl})]^{+}$ (1809, 100)
$\mathbf{1} + \mathrm{SnBuCl_3}$	20–40	$[\mathbf{1}(\mathrm{SnBuCl})]^{2+}$ (904, 100), $[\mathbf{1}(\mathrm{SnBuCl_2})]^{+}$ (1844, 5)
	60	$[\mathbf{1}(\mathrm{SnBuCl})]^{2+}$ (904, 100), $[\mathbf{1}(\mathrm{SnBuCl_2})]^{+}$ (1844, 20)
	80	$[\mathbf{1}(\mathrm{SnBuCl_2})]^{+}$ (1844, 100)
$\mathbf{1} + \mathrm{SnBu_2Cl_2}$	20	$[\mathbf{1}(\mathrm{SnBu_2})]^{2+}$ (915, 100), $[\mathbf{1}(\mathrm{SnBu_2Cl})]^{+}$ (1865, 51)
	40	$[\mathbf{1}(\mathrm{SnBu_2})]^{2+}$ (915, 100), $[\mathbf{1}(\mathrm{SnBu_2Cl})]^{+}$ (1865, 81)
	60	$[\mathbf{1}(\mathrm{SnBu_2})]^{2+}$ (915, 25), $[\mathbf{1}(\mathrm{SnBu_2Cl})]^{+}$ (1865, 100)
	80	$[(\mathbf{1} - \mathrm{PPh_3})(\mathrm{SnBu_2Cl})]^{+}$ (1603, 25), $[\mathbf{1}(\mathrm{SnBu_2Cl})]^{+}$ (1865, 100)
$\mathbf{1} + \mathrm{SnPhCl_3}$	20–40	$[\mathbf{1}(\mathrm{SnPhCl})]^{2+}$ (914, 100), $[\mathbf{1}(\mathrm{SnPhCl_2})]^{+}$ (1864, 3)
	60	$[\mathbf{1}(\mathrm{SnPhCl})]^{2+}$ (914, 100), $[\mathbf{1}(\mathrm{SnPhCl_2})]^{+}$ (1864, 17)
	80	$[\mathbf{1}(\mathrm{SnPhCl_2})]^{+}$ (1864, 100)
$\mathbf{1} + \mathrm{SnPh_2Cl_2}$	20	$[\mathbf{1}(\mathrm{SnPh_2})]^{2+}$ (935, 100), $[\mathbf{1}(\mathrm{SnPh_2Cl})]^{+}$ (1906, 70)
	40–60	$[\mathbf{1}(\mathrm{SnPh_2})]^{2+}$ (935, 30), $[\mathbf{1}(\mathrm{SnPh_2Cl})]^{+}$ (1906, 100)
	80	$[\mathbf{1}(\mathrm{SnPh_2})]^{2+}$ (935, 15), $[(\mathbf{1} - \mathrm{PPh_3})(\mathrm{SnPh_2Cl})]^{+}$ (1644, 10), $[\mathbf{1}(\mathrm{SnPh_2Cl})]^{+}$ (1906, 100)
	100	$[(\mathbf{1} - \mathrm{PPh_3})(\mathrm{SnPh_2Cl})]^{+}$ (1644, 100), $[\mathbf{1}(\mathrm{SnPh_2Cl})]^{+}$ (1906, 71)
$\mathbf{1} + \mathrm{SnPh_3Cl}$	20	$[\mathbf{1}(\mathrm{SnPh_2})]^{2+}$ (935, 39), $[\mathbf{1}(\mathrm{SnPh_2Cl})]^{+}$ (1906, 16), $[\mathbf{1}(\mathrm{SnPh_3})]^{+}$ (1947, 100)
	60	$[\mathbf{1}(\mathrm{SnPh_2})]^{2+}$ (935, 21), $[\mathbf{1}(\mathrm{SnPh_2Cl})]^{+}$ (1906, 30), $[\mathbf{1}(\mathrm{SnPh_3})]^{+}$ (1947, 100)
	80	$[(\mathbf{1} - \mathrm{PPh_3})(\mathrm{SnPh_2Cl})]^{+}$ (1644, 8), $[(\mathbf{1} - \mathrm{PPh_3})(\mathrm{SnPh_3})]^{+}$ (1685, 80), $[\mathbf{1}(\mathrm{SnPh_2Cl})]^{+}$ (1906, 31), $[\mathbf{1}(\mathrm{SnPh_3})]^{+}$ (1947, 100)
	100–120	$[(\mathbf{1} - \mathrm{PPh_3})(\mathrm{SnPh_2Cl})]^{+}$ (1644, 20), $[(\mathbf{1} - \mathrm{PPh_3})(\mathrm{SnPh_3})]^{+}$ (1685, 100), $[\mathbf{1}(\mathrm{SnPh_2Cl})]^{+}$ (1906, 3), $[\mathbf{1}(\mathrm{SnPh_3})]^{+}$ (1947, 13)
$\mathbf{1} + \mathrm{Sn(CH_2Ph)_2Br_2}$	20	$[\mathbf{1}(\mathrm{Sn(CH_2Ph)_2})]^{2+}$ (949, 100), $[\mathbf{1}(\mathrm{Sn(CH_2Ph)_2Br})]^{+}$ (1978, 58)
	40	$[\mathbf{1}(\mathrm{Sn(CH_2Ph)_2})]^{2+}$ (949, 100), $[\mathbf{1}(\mathrm{Sn(CH_2Ph)_2Br})]^{+}$ (1978, 78)
	60	$[\mathbf{1}(\mathrm{Sn})]^{2+}$ (858, 88), $[\mathbf{1}(\mathrm{Sn(CH_2Ph)_2})]^{2+}$ (949, 20), $[\mathbf{1}\mathrm{Sn(CH_2Ph)_2Br})]^{+}$ (1978, 100)
	80	$[\mathbf{1}(\mathrm{Sn})]^{2+}$ (858, 88), $[\mathbf{1}(\mathrm{Sn(CH_2Ph)_2})]^{2+}$ (949, 8), $[\mathbf{1}\mathrm{Sn(CH_2Ph)_2Br})]^{+}$ (1978, 100)

$\mathrm{(PPh_3)_4(SnMe_2Cl)][PF_6]}$ **5b**, $[\mathrm{Pt_2(\mu_3\text{-}Se)_2(PPh_3)_4(SnBuCl_2)][PF_6]}$ **7a**·3.5CHCl$_3$ and $[\mathrm{Pt_2(\mu_3\text{-}Se)_2(PPh_3)_4(SnBu_2Cl)][PF_6]}$ **7b** are given in Table 5, while pertinent bond distances and angles are in Tables 2–4. Figs. 3–5 illustrate the cationic structures of all the compounds with atomic numbering schemes. Fig. 3 shows the structure of the cationic aggregate of **5b**. X-Ray analysis revealed that it consists of an $\{\mathrm{SnMe_2Cl}\}$ moiety coordinated to the metalloligand $[\mathrm{Pt_2(\mu\text{-}Se)_2(PPh_3)_4}]$, forming a distorted square-based pyramidal aggregate. The two central Pt$^{\mathrm{II}}$ are slightly distorted from ideal square-planar geometry. The average Pt–Se–Pt bond angle in $[\mathrm{Pt_2(\mu\text{-}Se)_2(PPh_3)_4}]$ is 100.39°[10] but upon coordination to the $\{\mathrm{SnMe_2Cl}\}$ moiety it reduces to 88.53°. This closes the two platinum planes from near planar to a hinged conformation (130.8°), consistent with the theoretical calculations reported by Bencini *et al.*[10]

The structure of compound **7a**·3.5CHCl$_3$ is shown in Fig. 4. It shows significant disorder of the $\mathrm{PF_6}^-$ anion and the 3.5 CHCl$_3$ solvates in four regions of the asymmetric unit. For the disorder of the F atoms two models were resolved with occupancies of 0.7/0.3 and common isotropic thermal parameters were refined. Compound **7a** adopts a distorted square-based pyramidal structure with the Sn atom making an acute angle of 72.46° with the two Se atoms. Upon coordination to the $\{\mathrm{SnBuCl_2}\}$ moiety the $\{\mathrm{Pt_2Se_2}\}$ core bends from planarity, giving a dihedral angle of 128.0°. The C–Sn–Se bond angle of compound **7a** (96.7°) is only slightly (≈2%) higher than that of **5b** (94.6°), consistent with the minimal effect imparted by the larger $^{\mathrm{n}}$Bu group.

Table 2 Selected bond lengths [Å] and angles [°] for compound **5b**

Pt(1)–P(1)	2.2945(12)	Pt(2)–P(3)	2.3128(11)
Pt(1)–P(2)	2.3211(11)	Pt(2)–P(4)	2.2918(12)
Pt(1)–Se(1)	2.5030(5)	Pt(2)–Se(1)	2.4532(4)
Pt(1)–Se(2)	2.4858(4)	Pt(2)–Se(2)	2.4896(5)
Sn(1)–C(1)	2.138(4)	Sn(1)–Se(1)	2.7943(5)
Sn(1)–C(2)	2.137(5)	Sn(1)–Se(2)	2.6316(6)
Sn(1)–Cl(1)	2.4885(14)		
		Se(1)–Sn(1)–Se(2)	71.743(15)
Pt(1)–Se(1)–Pt(2)	88.740(15)	C(1)–Sn(1)–C(2)	112.1(2)
Pt(1)–Se(2)–Pt(2)	88.315(15)	C(1)–Sn(1)–Cl(1)	93.21(14)
Se(1)–Pt(1)–Se(2)	79.264(15)	C(2)–Sn(1)–Cl(1)	94.22(17)
Se(1)–Pt(2)–Se(2)	80.147(15)	Sn(1)–Se(1)–Pt(1)	76.918(14)
P(1)–Pt(1)–Se(1)	171.11(3)	Sn(1)–Se(1)–Pt(2)	86.187(15)
P(1)–Pt(1)–Se(2)	92.25(3)	Sn(1)–Se(2)–Pt(1)	80.330(14)
P(2)–Pt(1)–Se(1)	88.21(3)	Sn(1)–Se(2)–Pt(2)	89.088(16)
P(2)–Pt(1)–Se(2)	167.03(3)	C(1)–Sn(1)–Se(1)	94.73(14)
P(3)–Pt(2)–Se(1)	170.10(3)	C(1)–Sn(1)–Se(2)	130.34(14)
P(3)–Pt(2)–Se(2)	90.07(3)	C(2)–Sn(1)–Se(1)	101.67(16)
P(4)–Pt(2)–Se(1)	91.11(3)	C(2)–Sn(1)–Se(2)	117.36(15)
P(4)–Pt(2)–Se(2)	170.05(3)	Cl(1)–Sn(1)–Se(1)	158.03(5)
P(1)–Pt(1)–P(2)	100.40(4)	Cl(1)–Sn(1)–Se(2)	87.55(4)
P(3)–Pt(2)–P(4)	98.77(4)		

The cationic structure of **7b** (Fig. 5) shows the coordination of the metalloligand $[\mathrm{Pt_2(\mu\text{-}Se)_2(PPh_3)_4}]$ to the $\{\mathrm{SnBu_2Cl}\}$ fragment with the butyl groups on the Sn atom pointing away from one another, as well as from the phenyl rings on the $\{\mathrm{Pt_2Se_2}\}$ core. This arrangement maximizes the space above the $\{\mathrm{Pt_2Se_2}\}$ core, which promotes free orientation of the butyl groups and minimizes negative interaction between the phenyl rings.

Conclusion

We have demonstrated the powerful ability of ESMS in monitoring reactions that take advantage of the Lewis basicity of

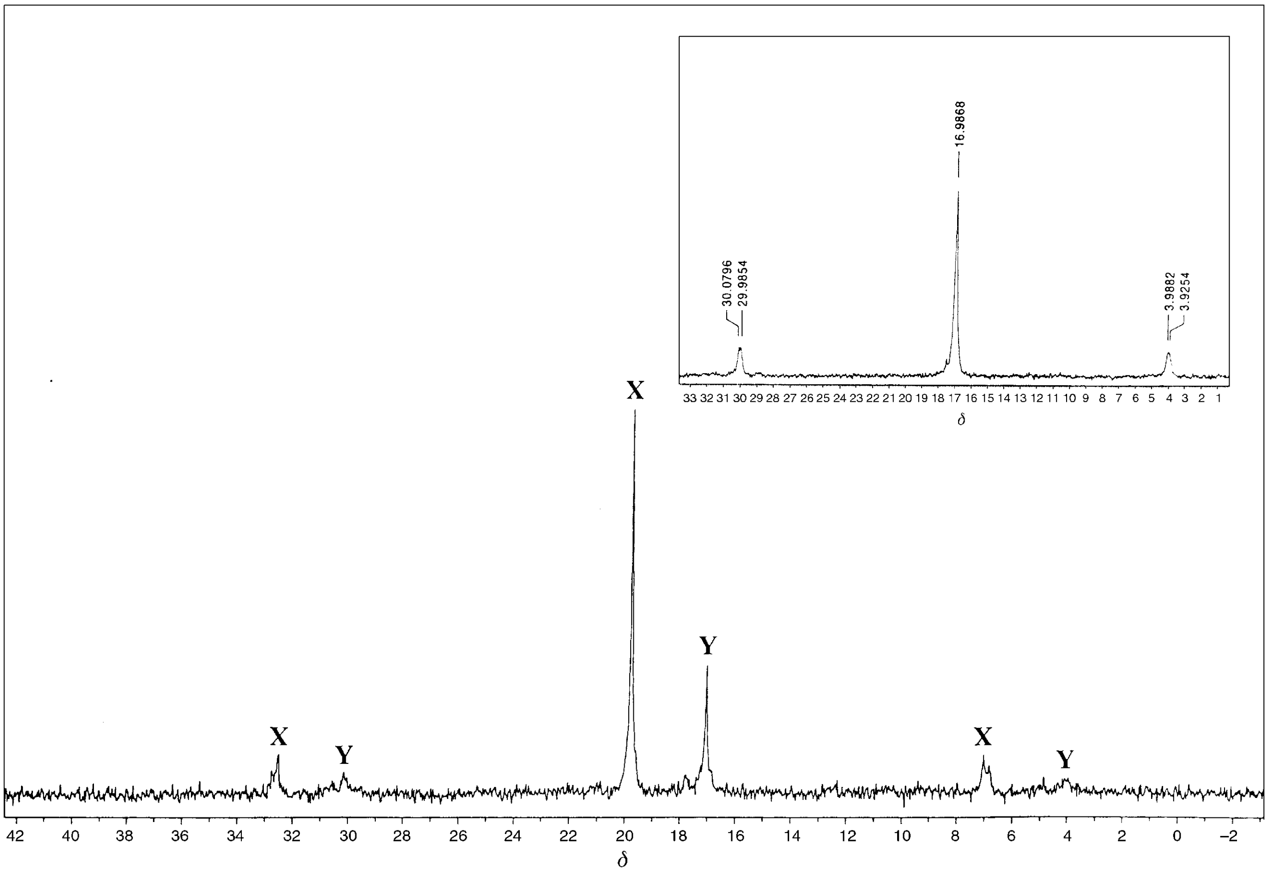

Fig. 2 ^{31}P-{H} NMR spectrum (recorded at 121.39 MHz with 85% H_3PO_4 as external reference) of the products isolated from the reaction between complex **1** and $SnPh_3Cl$, showing [**1**($SnPh_3$)][PF_6] (marked as X) and impurity [**1**($SnPh_2Cl$)][PF_6] (marked as Y). The inset shows the spectrum of [**1**($SnPh_2Cl$)][PF_6].

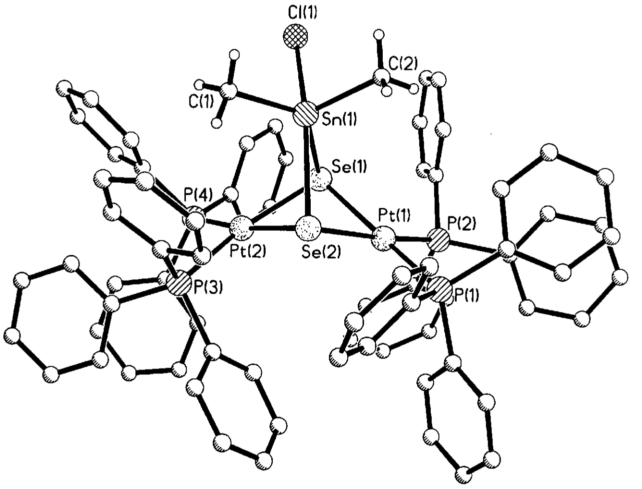

Fig. 3 Molecular structure of the cationic complex [$Pt_2(\mu_3\text{-}Se)_2(PPh_3)_4(SnMe_2Cl)$][$PF_6$] **5b**. The hydrogen atoms on the phenyl ligands and the PF_6^- counter ion are omitted for clarity.

selenide in [$Pt_2(\mu\text{-}Se)_2(PPh_3)_4$]. Upon mixing of the substrates, the technique is used to check whether a reaction is spontaneously feasible and the number of major products formed. As the reaction proceeds it offers an *in situ* analysis till the stage when the product is isolated. This form of "on-line" analysis of solution behavior is exemplified through successful displacement experiments of various tin(IV) organometallic substrates on [$Pt_2(\mu\text{-}Se)_2(PPh_3)_4$] and their subsequent isolation in bench-top syntheses. These results suggested that there is a clear link between ESMS behavior and synthetic realism, at least in this class of compounds. It is our hope that more synthetic chemists will take advantage of this technique to develop new species that are thought to be "transient".

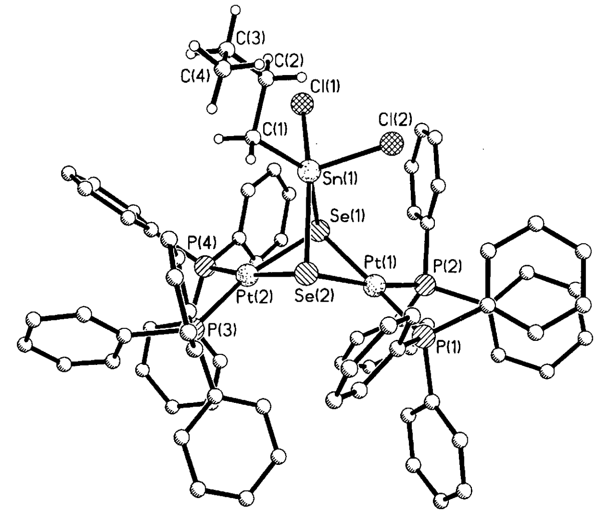

Fig. 4 Molecular structure of the cationic complex [$Pt_2(\mu_3\text{-}Se)_2(PPh_3)_4(SnBuCl_2)$][$PF_6$] **7a**. The chloroform solvate, PF_6^- counter ion and hydrogen atoms on the phenyl ligands are omitted for clarity.

Experimental

Mass spectrometry

Samples for ESMS analysis were prepared by dissolving complex **1** and substrate (both 10–100 μg) in 1 mL MeOH. Electrospray mass spectra were obtained with a VG Platform II mass spectrometer with the methanol mobile phase driven at 0.02 mL min^{-1} using a Thermo Separation products SpectraSystem P1000 LC pump. Samples were injected *via* a Rheodyne valve fitted with a 10 μL sample loop. The source temperature was 60 °C. The capillary potential tip was 3500 V, with nitrogen used both as drying and nebulizing gas. The skimmer cone

Table 3 Selected bond lengths [Å] and angles [°] for compound **7a**·3.5CHCl$_3$

Pt(1)–P(1)	2.320(2)	Pt(2)–P(3)	2.319(2)
Pt(1)–P(2)	2.295(2)	Pt(2)–P(4)	2.310(2)
Pt(1)–Se(1)	2.4853(9)	Pt(2)–Se(1)	2.4850(8)
Pt(1)–Se(2)	2.4719(8)	Pt(2)–Se(2)	2.5054(8)
Sn(1)–C(1)	2.161(11)	Sn(1)–Se(1)	2.5993(11)
Sn(1)–Cl(1)	2.457(3)	Sn(1)–Se(2)	2.8096(11)
Sn(1)–Cl(2)	2.387(3)		
Pt(1)–Se(1)–Pt(2)	86.98(3)	Se(1)–Sn(1)–Se(2)	72.46(3)
Pt(1)–Se(2)–Pt(2)	86.83(3)	C(1)–Sn(1)–Cl(1)	95.7(4)
Se(1)–Pt(1)–Se(2)	80.45(3)	C(1)–Sn(1)–Cl(2)	103.7(4)
Se(1)–Pt(2)–Se(2)	79.80(3)	Cl(1)–Sn(1)–Cl(2)	94.63(12)
P(1)–Pt(1)–Se(1)	88.34(7)	Sn(1)–Se(1)–Pt(1)	89.02(3)
P(1)–Pt(1)–Se(2)	168.74(7)	Sn(1)–Se(1)–Pt(2)	82.63(3)
P(2)–Pt(1)–Se(1)	172.22(6)	Sn(1)–Se(2)–Pt(1)	84.67(3)
P(2)–Pt(1)–Se(2)	92.06(6)	Sn(1)–Se(2)–Pt(2)	78.12(3)
P(3)–Pt(2)–Se(1)	165.94(6)	C(1)–Sn(1)–Se(1)	144.0(4)
P(3)–Pt(2)–Se(2)	88.13(6)	C(1)–Sn(1)–Se(2)	96.7(3)
P(4)–Pt(2)–Se(1)	91.19(6)	Cl(1)–Sn(1)–Se(1)	86.75(9)
P(4)–Pt(2)–Se(2)	170.51(6)	Cl(1)–Sn(1)–Se(2)	157.79(9)
P(1)–Pt(1)–P(2)	99.11(8)	Cl(2)–Sn(1)–Se(1)	111.87(8)
P(3)–Pt(2)–P(4)	101.18(8)	Cl(2)–Sn(1)–Se(2)	99.26(8)

Table 4 Selected bond lengths [Å] and angles [°] for compound **7b**

Pt(1)–P(1)	2.314(2)	Pt(2)–P(3)	2.301(2)
Pt(1)–P(2)	2.285(2)	Pt(2)–P(4)	2.288(2)
Pt(1)–Se(1)	2.4663(9)	Pt(2)–Se(1)	2.4599(9)
Pt(1)–Se(2)	2.4969(8)	Pt(2)–Se(2)	2.4897(8)
Sn(1)–C(1)	2.141(9)	Sn(1)–Se(1)	2.9349(10)
Sn(1)–C(5)	2.124(10)	Sn(1)–Se(2)	2.5919(11)
Sn(1)–Cl(1)	2.475(3)		
Pt(1)–Se(1)–Pt(2)	87.59(3)	P(4)–Pt(2)–Se(2)	93.80(5)
Pt(1)–Se(2)–Pt(2)	86.26(3)	P(1)–Pt(1)–P(2)	99.02(6)
Se(1)–Pt(1)–Se(2)	79.67(3)	P(3)–Pt(2)–P(4)	98.56(6)
Se(1)–Pt(2)–Se(2)	79.94(3)	Se(1)–Sn(1)–Se(2)	69.93(3)
P(1)–Pt(1)–Se(1)	169.35(4)	C(1)–Sn(1)–C(5)	116.7(5)
P(1)–Pt(1)–Se(2)	89.73(5)	C(1)–Sn(1)–Cl(1)	94.8(3)
P(2)–Pt(1)–Se(1)	91.61(5)	C(5)–Sn(1)–Cl(1)	97.9(4)
P(2)–Pt(1)–Se(2)	170.70(5)	Sn(1)–Se(1)–Pt(1)	81.10(3)
P(3)–Pt(2)–Se(1)	88.64(5)	Sn(1)–Se(1)–Pt(2)	81.94(3)
P(3)–Pt(2)–Se(2)	166.11(4)	Sn(1)–Se(2)–Pt(1)	87.80(3)
P(4)–Pt(2)–Se(1)	169.95(5)	Sn(1)–Se(2)–Pt(2)	88.77(3)

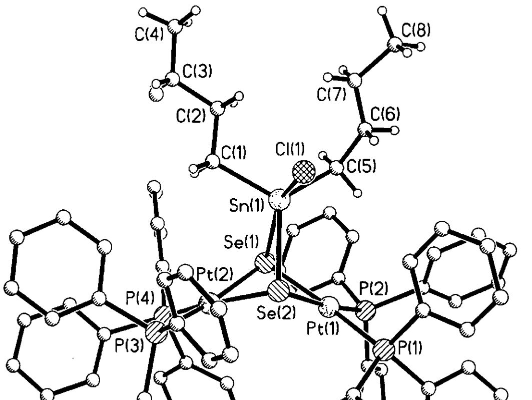

Fig. 5 Molecular structure of the cationic complex [Pt$_2$(μ$_3$-Se)$_2$(PPh$_3$)$_4$-(SnBu$_2$Cl)][PF$_6$] **7b**. Details as in Fig. 3.

voltage was usually 5 V when clean parent ions were required, and was varied up to 80 V to investigate fragmentation processes. Peaks were assigned from the *m/z* values and from the isotope distribution patterns that were simulated using the ISOTOPE program.[11] The *m/z* values given are for the most intense peak in the envelope in each case.

Materials

The substrates used for analysis were SnMeCl$_3$, SnMe$_2$Cl$_2$, SnMe$_3$Cl, SnEt$_2$Cl$_2$, SnBuCl$_3$, SnBu$_2$Cl$_2$, SnPhCl$_3$, SnPh$_2$Cl$_2$, SnPh$_3$Cl and Sn(CH$_2$Ph)$_2$Br$_2$, all commercially available from Strem except for SnEt$_2$Cl$_2$[12] and Sn(CH$_2$Ph)$_2$Br$_2$.[13] All reactions were performed under a positive pressure of purified Ar unless otherwise stated, and solvents were distilled and degassed before use. ^{1}H NMR spectra were recorded at 300 MHz at 25 °C on a Bruker ACF 300 spectrometer. Chemical shifts are reported in ppm to high frequency with Me$_4$Si as internal standard. The ^{31}P NMR spectra were recorded at 121.39 MHz with 85% H$_3$PO$_4$ as external reference. Elemental analyses were performed by the microanalytical laboratory of the Department of Chemistry at the National University of Singapore.

[Pt$_2$(μ-Se)$_2$(PPh$_3$)$_4$] **1** was prepared by a modification of the literature method.[10] To a stirred mixture of Se (1.840 g, 23.31 mmol) in deionized and deoxygenated water (40 mL) was added NaBH$_4$ (1.014 g, 26.77 mmol)[14] at *ca.* 0 °C. After 15 min the colorless solution of NaHSe was transferred to a benzene suspension (50 mL) of *cis*-[PtCl$_2$(PPh$_3$)$_2$][15] (4.742 g, 6.00 mmol) under N$_2$. The suspension turned yellow and then darkened to brown after a day. This suspension was filtered and the solid was washed successively with deionized water and MeOH (100 mL) and dried (yield = 4.653 g, 49%). ^{31}P-{^{1}H} NMR (d$_7$-DMF): δ_P 10.2 [t, ^1J(P–Pt) = 3889 Hz].

Synthesis of Pt–Se–Sn aggregates

[Pt$_2$(μ$_3$-Se)$_2$(PPh$_3$)$_4$(SnMeCl$_2$)][PF$_6$] 5a. SnMeCl$_3$ (7.2 mg, 0.0299 mmol) was added to a brown suspension of complex **1** (47.6 mg, 0.0298 mmol) in MeOH (20 mL). The resultant bright yellow solution was stirred for 3 h, after which an excess of NH$_4$PF$_6$ (10.0 mg, 0.0614 mol) was introduced to give a light yellow suspension. After stirring for 1 h, deionized water (50 mL) was added to induce precipitation. The suspension was filtered, the solid washed successively with 100 mL portions of deionized water and Et$_2$O, and dried under vacuum yielding a light yellow powder of **5a** (0.0285 g, 49%). Found: C, 44.7; H, 3.3; P, 7.8. Calc. for C$_{73}$H$_{63}$Cl$_2$F$_6$P$_5$Pt$_2$Se$_2$Sn: C, 45.0; H, 3.3; P, 8.0%. ^{31}P-{^{1}H} NMR (CDCl$_3$): δ_P 16.9 [t, ^1J(P–Pt) = 3212 Hz]. ^{1}H NMR (CDCl$_3$): δ_H 1.28 (s, 3H, CH$_3$) and 7.08–7.45 (m, 60H, 12C$_6$H$_5$).

[Pt$_2$(μ$_3$-Se)$_2$(PPh$_3$)$_4$(SnMe$_2$Cl)][PF$_6$] 5b. A similar procedure to that described above using SnMe$_2$Cl$_2$ (7.1 mg, 0.0323 mmol) and complex **1** (51.1 mg, 0.0320 mmol) gave a yellow-brown powder of **5b** (0.0209 g, 34%). Found: C, 46.0; H, 3.5; P, 7.6. Calc. for C$_{74}$H$_{66}$ClF$_6$P$_5$Pt$_2$Se$_2$Sn: C, 46.1; H, 3.5; P, 8.0%. ^{31}P-{^{1}H} NMR (CDCl$_3$): δ_P 17.6 [t, ^1J(P–Pt) = 3151 Hz]. ^{1}H NMR (CDCl$_3$): δ_H 1.30 (s, 6H, 2CH$_3$) and 7.08–7.50 (m, 60H, 12C$_6$H$_5$).

[Pt$_2$(μ$_3$-Se)$_2$(PPh$_3$)$_4$(SnMe$_3$)][PF$_6$] 5c. Similarly, SnMe$_3$Cl (6.0 mg, 0.0301 mmol) and complex **1** (47.7 mg, 0.0299 mmol) gave a yellow powder of **5c** (0.0337 g, 59%). Found: C, 47.0; H, 3.8; P, 7.9. Calc. for C$_{75}$H$_{69}$F$_6$P$_5$Pt$_2$Se$_2$Sn: C, 47.3; H, 3.9; P, 8.1%. ^{31}P-{^{1}H} NMR (CDCl$_3$): δ_P 21.0 [t, ^1J(P–Pt) = 3037 Hz]. ^{1}H NMR (CDCl$_3$): δ_H 1.32 (s, 9H, 3CH$_3$) and 6.93–7.80 (m, 60H, 12C$_6$H$_5$).

[Pt$_2$(μ$_3$-Se)$_2$(PPh$_3$)$_4$(SnEt$_2$Cl)][PF$_6$] 6. Similarly, SnEt$_2$Cl$_2$ (7.5 mg, 0.0303 mmol) and complex **1** (48.4 mg, 0.0303 mmol) gave a brown powder of **6** (0.0228 g, 38%). Found: C, 45.5; H, 3.4; P, 7.8. Calc. for C$_{74}$H$_{65}$ClF$_6$P$_5$Pt$_2$Se$_2$Sn: C, 45.5; H, 3.4; P, 7.9%.

Table 5 Crystallographic data for complexes **5b**, **7a** and **7b**

	5b	**7a**·3.5CHCl$_3$	**7b**
Formula	$C_{74}H_{66}ClF_6P_5Pt_2Se_2Sn$	$C_{79.5}H_{72.5}Cl_{12.5}F_6P_5Pt_2Se_2Sn$	$C_{80}H_{78}ClF_6P_5Pt_2Se_2Sn$
Formula weight	1926.360	2406.664	2010.597
Crystal system	Monoclinic	Triclinic	Triclinic
Space group	$P2_1/c$	$P\bar{1}$	$P\bar{1}$
a/Å	20.2150(3)	14.4249(2)	12.337(2)
b/Å	19.524(1)	16.5335(2)	16.102(5)
c/Å	18.0565(3)	21.0858(3)	21.258(5)
α/°		69.018(1)	86.54(2)
β/°	91.88(1)	84.323(1)	86.82(2)
γ/°		86.547(1)	87.80(2)
V/Å^3	7122.52(16)	4670.7(1)	4206.1(17)
Z	4	2	2
μ/mm^{-1}	5.496	4.527	4.947
T/K	203(2)	203(2)	223(2)
No. unique reflections	34409	32947	30600
No. observed reflections [$I > 2\sigma(I)$]	13100	15617	18652
R	0.0345	0.0513	0.0427
wR	0.0553	0.1359	0.1211

^{31}P-{^{1}H} NMR (CDCl$_3$): δ_P 17.4 [t, ^1J(P–Pt) = 3155 Hz]. ^{1}H NMR (CDCl$_3$): δ_H 1.27 (t, 6H, 2CH$_3$), 2.32 (q, 4H, 2CH$_2$) and 7.12–7.34 (m, 60H, 12C$_6$H$_5$).

[Pt$_2$(μ$_3$-Se)$_2$(PPh$_3$)$_4$(SnBuCl$_2$)][PF$_6$] 7a. Similarly, SnBuCl$_3$ (14.9 mg, 8.78 μL, 0.0312 mmol) and complex **1** (49.6 mg, 0.0311 mmol) gave a pale yellow powder of **7a** (0.0474 g, 77%). Found: C, 46.0; H, 3.5; P, 7.8. Calc. for $C_{76}H_{69}Cl_2F_6P_5Pt_2Se_2Sn$: C, 45.9; H, 3.5; P, 7.8%. ^{31}P-{^{1}H} NMR (CDCl$_3$): δ_P 16.9 [t, ^1J(P–Pt) = 3216 Hz]. ^{1}H NMR (CDCl$_3$): δ_H 0.85 (t, 3H, CH$_3$), 1.26–1.35 (m, 4H, 2CH$_2$), 1.99 (t, 2H, CH$_2$) and 7.16–7.32 (m, 60H, 12C$_6$H$_5$).

[Pt$_2$(μ$_3$-Se)$_2$(PPh$_3$)$_4$(SnBu$_2$Cl)][PF$_6$] 7b. Similarly, SnBu$_2$Cl$_2$ (9.7 mg, 0.0319 mmol) and complex **1** (50.5 mg, 0.0316 mmol) gave a light brown powder of **7b** (0.0356 g, 56%). Found: C, 47.7; H, 3.9; P, 7.7. Calc. for $C_{80}H_{78}ClF_6P_5Pt_2Se_2Sn$: C, 47.8; H, 3.9; P, 7.7%. ^{31}P-{^{1}H} NMR (CDCl$_3$): δ_P 17.5 [t, ^1J(P–Pt) = 3166 Hz]. ^{1}H NMR (CDCl$_3$): δ_H 0.88 (t, 6H, 2CH$_3$), 1.18–1.33 (m, 8H, 4CH$_2$), 1.92 (t, 4H, 2CH$_2$) and 7.12–7.32 (m, 60H, 12C$_6$H$_5$).

[Pt$_2$(μ$_3$-Se)$_2$(PPh$_3$)$_4$(SnPhCl$_2$)][PF$_6$] 8a. Similarly, SnPhCl$_3$ (17.8 mg, 9.68 μL, 0.0320 mmol) and complex **1** (50.8 mg, 0.0318 mmol) gave a pale yellow powder of **8a** (0.0347 g, 54%). Found: C, 46.2; H, 3.2; P, 7.5. Calc. for $C_{78}H_{65}Cl_2F_6P_5Pt_2Se_2Sn$: C, 46.6; H, 3.3; P, 7.7%. ^{31}P-{^{1}H} NMR (CDCl$_3$): δ_P 16.7 [t, ^1J(P–Pt) = 3223 Hz]. ^{1}H NMR (CDCl$_3$): δ_H 7.11–7.33 (m, 60H, 12C$_6$H$_5$) and 7.48–7.76 (m, 5H, C$_6$H$_5$ on Sn).

[Pt$_2$(μ$_3$-Se)$_2$(PPh$_3$)$_4$(SnPh$_2$Cl)][PF$_6$] 8b. Similarly, SnPh$_2$Cl$_2$ (10.1 mg, 0.0294 mmol) and complex **1** (46.5 mg, 0.0291 mmol) gave a yellow powder of **8b** (0.0342 g, 57%). Found: C, 49.0; H, 3.4; P, 7.5. Calc. for $C_{84}H_{70}ClF_6P_5Pt_2Se_2Sn$: C, 49.2; H, 3.4; P, 7.6%. ^{31}P-{^{1}H} NMR (CDCl$_3$): δ_P 17.0 [t, ^1J(P–Pt) = 3178 Hz]. ^{1}H NMR (CDCl$_3$): δ_H 7.06–7.31 (m, 60H, 12C$_6$H$_5$) and 7.40–7.75 (m, 10H, 2C$_6$H$_5$ on Sn).

[Pt$_2$(μ$_3$-Se)$_2$(PPh$_3$)$_4$(SnPh$_3$)][PF$_6$] 8c. Similarly, SnPh$_3$Cl (11.5 mg, 0.0298 mmol) and complex **1** (46.9 mg, 0.0294 mmol) gave a brown powder of **8c** (0.0229 g, 37%). ^{31}P-{^{1}H} NMR (CDCl$_3$): δ_P 19.8 [t, ^1J(P–Pt) = 3124] and 17.0 [t, ^1J(P–Pt) = 3178 Hz] (contamination of SnPh$_2$Cl$_2$ in substrate resulted in formation of **8b**). ^{1}H NMR (CDCl$_3$): δ_H 7.06–7.31 (m, 120H, 24C$_6$H$_5$ from **8b** and **8c**) and 7.40–7.75 (m, 25H, 2C$_6$H$_5$ from **8b** and 3C$_6$H$_5$ from **8c**).

[Pt$_2$(μ$_3$-Se)$_2$(PPh$_3$)$_4${Sn(CH$_2$Ph)$_2$Br}][PF$_6$] 9. Similarly, Sn(CH$_2$Ph)$_2$Br$_2$ (14.5 mg, 0.0315 mmol) and complex **1** (50.2 mg, 0.0314 mmol) gave a yellow powder of **9** (0.0388 g, 58%). Found: C, 48.8; H, 3.5; P, 7.5. Calc. for $C_{86}H_{74}BrF_6P_5Pt_2Se_2Sn$: C, 48.7; H, 3.5; P, 7.3%. ^{31}P-{^{1}H} NMR (CDCl$_3$): δ_P 17.5 [t, ^1J(P–Pt) = 3143 Hz]. ^{1}H NMR (CDCl$_3$): δ_H 3.14 (d, 2H, PhCH$_2$), 3.44 (d, 2H, PhCH$_2$), 6.50–6.68 (m, 10H, C$_6$H$_5$CH$_2$) and 7.03–7.35 (m, 60H, 12C$_6$H$_5$).

Crystal structure determination and refinement

The data collection was performed on a Bruker AXS SMART diffractometer, equipped with a CCD area-detector using Mo-Kα radiation (λ = 0.71073 Å). The software SMART[16] was used for collecting frames of data, indexing reflections, and the determination of lattice parameters, SAINT[16] for integration of intensity of reflections and scaling, SADABS[17] for empirical absorption correction, and SHELXTL[18] for space group and structure determination, refinements, graphics, and structure reporting. Hydrogen atoms were not located. The structures were refined by full-matrix least squares on F^2 with anisotropic thermal parameters for non-hydrogen atoms, unless otherwise indicated. A summary of parameters for the data collections and refinements is given in Table 5.

Suitable single crystals of [Pt$_2$(μ$_3$-Se)$_2$(PPh$_3$)$_4$(SnMe$_2$Cl)][PF$_6$] **5b** and [Pt$_2$(μ$_3$-Se)$_2$(PPh$_3$)$_4$(SnBu$_2$Cl)][PF$_6$] **7b** were obtained by layering a CH$_2$Cl$_2$ solution of each compound with hexane, while those of [Pt$_2$(μ$_3$-Se)$_2$(PPh$_3$)$_4$(SnBuCl$_2$)][PF$_6$]·3.5CHCl$_3$ **7a** were obtained by layering a CHCl$_3$ solution with hexane. For **7a**·3.5CHCl$_3$ the F atoms in the PF$_6^-$ counter anion are disordered. Two models were resolved (occupancies 0.7/0.3) and common isotropic thermal parameters refined. There are 3.5 CHCl$_3$ solvate molecules present in four regions of the asymmetric unit, most of them being disordered. Common isotropic thermal parameters were refined for these non-hydrogen atoms in the solvent.

CCDC reference number 186/2276.

See http://www.rsc.org/suppdata/dt/b0/b006907h/ for crystallographic files in .cif format.

Acknowledgements

The authors acknowledge the National University of Singapore (NUS) for support (Grant RP 982755) and J. S. L. Y. thanks NUS for a research scholarship and for attachment to University of Waikato. W. H. thanks the University of Waikato and the New Zealand Lottery Grants Board for financial assistance, and Johnson-Matthey plc for a generous loan of platinum. We thank Professor Brian K. Nicholson for the supply of tin compounds and G. K. Tan for her assistance in X-ray analysis.

References

1 M. I. Bruce, *Adv. Organomet. Chem.*, 1968, **6**, 273; J. Lewis and B. F. G. Johnson, *Acc. Chem. Res.*, 1968, **1**, 245; M. R. Litzow and T. R. Spalding, *Mass Spectrometry of Inorganic and Organometallic Compounds*, Elsevier, Amsterdam, 1973.

2 (*a*) J. B. Fenn, M. Mann, C. K. Meng, S. F. Wong and C. M. Whitehouse, *Science*, 1989, **246**, 64; (*b*) J. B. Fenn, M. Mann, C. K. Meng, S. F. Wong and C. M. Whitehouse, *Mass Spectrom. Rev.*, 1990, **9**, 37.

3 I. I. Stewart, *Spectrochim. Acta*, *Part B*, 1999, **54**, 1649; R. B. Cole, *Electrospray Ionisation Mass Spectrometry; Fundamentals, Instrumentation and Applications*, Wiley-Interscience, New York, 1997; G. J. Langley and G. A. Mills, *Educ. Chem.*, 1997, 14; R. Bakhtiar, S. A. Hofstadler and R. D. Smith, *J. Chem. Educ.*, 1996, **73**, A118; M. Przybylski and M. O. Glocker, *Angew. Chem., Int. Ed. Engl.*, 1996, **35**, 807; M. Mann and M. Wilm, *Trends Biochem. Sci.*, 1995, **20**, 219; R. D. Smith, J. A. Loo, C. G. Edmonds, C. J. Barinaga and H. R. Udseth, *Mass Spectrom. Rev.*, 1991, **10**, 359.

4 B. F. G. Johnson and J. S. McIndoe, *Coord. Chem. Rev.*, 2000, **200**, 901; R. Colton, A. D'Agostino and J. C. Traeger, *Mass Spectrom. Rev.*, 1995, **14**, 79; I. I. Stewart and G. Horlick, *Trends Anal. Chem.*, 1996, **15**, 80; C. E. C. A. Hop and R. Bakhtiar, *J. Chem. Educ.*, 1996, **73**, A165; A. Canty, R. Colton and I. M. Thomas, *J. Organomet. Chem.*, 1993, **455**, 283; A. Canty and R. Colton, *Inorg. Chim. Acta*, 1994, **215**, 179; D. Dakternieks, H. Zhu, E. R. T. Tiekink and R. Colton, *J. Organomet. Chem.*, 1994, **476**, 33; W. Henderson and M. J. Taylor, *Polyhedron*, 1996, **15**, 1957; L. J. McCaffrey, W. Henderson, B. K. Nicholson, J. E. Mackay and M. B. Dinger, *J. Chem. Soc.*, *Dalton Trans.*, 1997, 2577.

5 W. Henderson, B. K. Nicholson and L. J. McCaffrey, *Polyhedron*, 1998, **17**, 4291.

6 S.-W. A. Fong, W. T. Yap, J. J. Vittal, A. G. Oliver, C. E. F. Rickard, W. Henderson and T. S. A. Hor, manuscript in preparation.

7 S.-W. A. Fong and T. S. A. Hor, *J. Chem. Soc.*, *Dalton Trans.*, 1999, 639.

8 A. Bencini and S. Midollini, *Coord. Chem. Rev.*, 1992, **120**, 87; L. C. Roof and J. W. Kolis, *Chem. Rev.*, 1993, **93**, 1037.

9 A. G. Davis and P. J. Smith, in *Comprehensive Organometallic Chemistry*, ed. G. Wilkinson, Pergamon Press, Oxford, 1982, vol. 2, ch. 11.11.3, p. 606.

10 A. Bencini, M. D. Vaira, R. Morassi and P. Stoppioni, *Polyhedron*, 1996, **15**, 2079.

11 L. J. Arnold, *J. Chem. Educ.*, 1992, **69**, 811.

12 R. J. Angelici, *Synthesis and Technique in Inorganic Chemistry*, W. B. Saunders Company, Philadelphia, 1969, p. 153.

13 Modifications from literature procedures, K. Sisido, Y. Takeda and Z. Kinugawa, *J. Am. Chem. Soc.*, 1961, **83**, 538.

14 D. L. Klayman and T. S. Griffin, *J. Am. Chem. Soc.*, 1973, **95**, 197.

15 G. Cavinato and L. Toniolo, *Inorg. Chim. Acta*, 1981, **52**, 39.

16 *SMART & SAINT Software Reference Manuals*, version 4.0, Siemens Energy & Automation, Inc., Analytical Instrumentation, Madison, WI, 1996.

17 G. M. Sheldrick, SADABS, software for empirical absorption correction, University of Göttingen, 1993.

18 G. M. Sheldrick, SHELXTL, version 5.03, Siemens Energy & Automation, Inc., Analytical Instrumentation, Madison, WI, 1996.